

# Cavity Ringdown Spectroscopy of the $\tilde{A} - \tilde{X}$ Electronic Transition of the Phenyl Peroxy Radical

Gabriel M. P. Just, Erin N. Sharp, Sergey J. Zalyubovsky, and Terry A. Miller

Laser Spectroscopy Facility

Department of Chemistry

The Ohio State University

120 W. 18th Avenue

Columbus Ohio 43210

fax: (614)292-1948, email: tamiller@chemistry.ohio-state.edu

August 31, 2005

## Abstract

Cavity ringdown spectra (CRDS) of the near IR  $\tilde{A}^2A' - \tilde{X}^2A''$  electronic transition of phenyl peroxy radical are reported. The electronic origin is observed at  $7497 \text{ cm}^{-1}$ . *Ab initio* calculations have been carried out to aid the assignment of the electronic origin and other bands involving vibrational excitation.

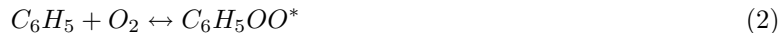
# 1 Introduction

The reaction of alkyl radicals with  $O_2$  is of great importance in the fields of atmospheric and combustion chemistry. Oxidation of hydrocarbons at low temperatures is a key process that occurs not only in the operation of internal combustion engines,<sup>1-3</sup> but also is present in the chemistry of the troposphere.<sup>4-8</sup> While oxidation can lead to a variety of final products, reactive intermediates such as peroxy radicals ( $RO_2\cdot$ ) are formed early on in the oxidation mechanism. They result from reacting alkyl radicals with molecular oxygen.<sup>7</sup>



The reaction of phenyl radical ( $C_6H_5$ ) with oxygen is of critical importance, in that it is believed to impede the formation of soot, which is inherent in hydrocarbon combustion reactions.<sup>9,10</sup> If phenyl radical is not further oxidized, then its recombination reactions can lead to larger unsaturated hydrocarbons that are precursors to soot.

Even if the oxidation reaction precedes its product distribution differs with temperature and pressure, e.g.,



Clearly Eqs. 3-5 provide important branching mechanism for combustion chain reactions. A theoretical study using RRKM methods<sup>11</sup> found that at relatively low temperatures ( $T < 1000$  K), the formation and stabilization of phenyl peroxy radicals dominates the reaction, while at higher temperatures, the production of phenoxy radical becomes competitive (Eq. 5). Indeed, the appearance of phenyl peroxy at lower oxidation temperatures (297-500 K) has been verified experimentally.<sup>11</sup>

Alkyl peroxy radicals, in general, have traditionally been studied by monitoring their  $\tilde{B}^2A'' - \tilde{X}^2A''$  electronic transition in the UV. This transition is typically centered around 240 nm, with a half width of

$\sim 40$  nm, and is characteristically broad and structureless due to the dissociative nature of the  $\tilde{B}$  state. Therefore, it is difficult to extract any useful rotational or vibrational information from the  $\tilde{B}-\tilde{X}$  transition, and in addition, the UV spectra of most alkyl peroxy radicals strongly overlap, making identification of a particular RO<sub>2</sub> species difficult. These same characteristics are expected for the  $\tilde{B}-\tilde{X}$  transition of phenyl peroxy as well, except that the transition is shifted from the UV to the visible, where a broad, structureless absorption has been reported<sup>11</sup> by CRDS spectroscopy.

Recently, research on the peroxy radicals has shifted its focus to the  $\tilde{A}^2A' - \tilde{X}^2A''$  IR transition, which was once thought of as too weak to observe spectroscopically as<sup>12,13</sup>  $\sigma \approx 2 \times 10^{-21}$  cm<sup>-2</sup>. However, the cavity ringdown spectroscopy (CRDS) technique has proven to be extremely useful in this application, and our group, in particular, has successfully studied this transition in methyl peroxy (CH<sub>3</sub>O<sub>2</sub>),<sup>13</sup> trifluoromethyl peroxy (CF<sub>3</sub>O<sub>2</sub>),<sup>14</sup> acetyl peroxy (CH<sub>3</sub>C(O)O<sub>2</sub>),<sup>15</sup> and propyl peroxy radical (C<sub>3</sub>H<sub>7</sub>O<sub>2</sub>)<sup>16</sup> radicals.

Despite the overwhelming relevance of the phenyl peroxy species, there has been little spectroscopic analysis to date, which would accurately characterize its ground and excited states. Herein, we report the first observation of the  $\tilde{A}^2A' - \tilde{X}^2A''$  transition of phenyl peroxy radical using our near infrared (NIR) CRDS apparatus. To facilitate spectroscopic assignment, *ab initio* calculations for the  $\tilde{A}$  and  $\tilde{X}$  states have been carried out in order to predict geometry, vibrational frequencies, and the origin frequency ( $T_{00}$ ) of this electronic transition.

## 2 Experimental

### 2.1 Apparatus Description

Our CRDS apparatus for studying the NIR transition of peroxy radicals has been described in detail previously.<sup>13</sup> In our experimental setup, IR radiation in the region 1.2-1.3  $\mu$ m was generated by a Raman shifting of the output of a dye laser in molecular hydrogen. A Nd:YAG pumped dye laser system (PRO-270, Spectra Physics; Sirah) was operated at 20Hz and was shifted into the NIR region via stimulated Raman scattering in gaseous H<sub>2</sub>. Operated with DCM and Rhodamine B laser dye(Exiton), the system produced 90-130 mJ/pulse of tunable radiation in the region of 594-637 nm with a linewidth of 0.06 cm<sup>-1</sup>. The output of the dye laser was focused by a lens (f=50 cm) into a 70 cm long single Raman cell filled with 200-300 psi of H<sub>2</sub>. The output radiation from the Raman cell was spectrally filtered using several 1.0  $\mu$ m cut-off longwave filters (Corion LL-1000-F) to eliminate antiStokes and first Stokes radiation. The resulting 1-2 mJ of the second Stokes radiation in the 1.2-1.3  $\mu$ m region was delivered to the ringdown cell through two 1 m focal length lenses. The ringdown cavity was fabricated of stainless steel and consists of a 20 cm long central part

with two rectangular UV grade quartz photolysis windows and two 15 cm long arms. The cavity ringdown mirrors (purchased from Los Gatos Research Inc.) were positioned at the ends of the arms on adjustable mounts. A Thorlabs InGaAs (PDA400) photodiode was used to detect the outgoing radiation, and its output was recorded by a 12 bit digitizing card (Measurement Computing) for further analysis.

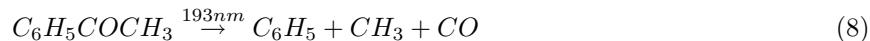
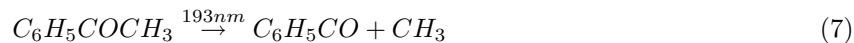
The photolysis excimer laser (LPX120icc, Lambda Physics) was operated at 193 nm, and the beam was shaped by cylindrical and spherical lenses to a rectangle (0.5×13 cm). The excimer laser was sent through the photolysis quartz windows into the central part of the flow cell. Background absorption of the precursors and residual water vapor were eliminated by the subtraction of data points taken with the excimer beam on and off for each laser step. Our NIR Raman shifted frequencies were calibrated using the HITRAN<sup>17</sup> database from water absorptions. Control of the lasers, experimental time sequence fitting procedure and the fitting of the data were all performed by a PC-based Labview data acquisition software.

## 2.2 Phenyl Peroxy Radical Production

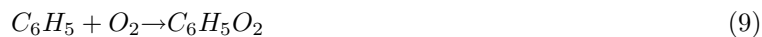
There are several precursors available that can produce the phenyl peroxy radical upon photolysis with 193 nm light followed by reaction with O<sub>2</sub>. In this study, we primarily used acetophenone (Aldrich) to produce phenyl radical according to the following pathway<sup>18</sup>



Two other dissociation pathways are also possible.



The first two channels (Eqs. 6 and 7) have comparable cross sections,<sup>18</sup> while that of the third channel (Eq. 8) is estimated to be less than 0.1 percent of the first two. Even though reactions 6 and 7 are equally favored in photolysis, 30-50 percent of C<sub>6</sub>H<sub>5</sub>CO, which is initially formed in reaction 7, further decomposes to C<sub>6</sub>H<sub>5</sub> + CO. Once phenyl radical is formed under our condition, it reacts with molecular oxygen to form phenyl peroxy radical.<sup>19-21</sup>



Another precursor available for the production of phenyl radical is bromobenzene (Aldrich). Similar to the production of phenyl peroxy radical described above for acetophenone, upon photolysis (193 nm) of bromobenzene, phenyl radical is formed.



Phenyl then reacts with O<sub>2</sub> to product C<sub>6</sub>H<sub>5</sub>O<sub>2</sub>. However, the absorption cross section for bromobenzene is expected to be smaller than that of acetophenone, making production of phenyl from C<sub>6</sub>H<sub>5</sub>Br somewhat less favorable than from C<sub>6</sub>H<sub>5</sub>COCH<sub>3</sub>. Therefore, bromobenzene was used as a precursor only to verify chemically the production of phenyl peroxy radical. Following this verification of the phenyl peroxy spectral features from both sources, acetophenone was preferentially used as a precursor in subsequent scans because it allowed us to check our sensitivity against the methyl peroxy radical signal, since methyl radical is also produced by photolysis (see Eq. 7).

In our experiment, we filled the ringdown cell with a mixture of 30 Torr of O<sub>2</sub>, 70 Torr of N<sub>2</sub> and about 0.3 Torr of precursor (acetophenone or bromobenzene). The photolysis pulse was fired approximately 90 μs before the dye laser allowing enough time for the peroxy radicals to form, but not enough time to allow for radical-radical recombination or other secondary reactions.

## 3 Results and Discussion

### 3.1 *Ab initio* Calculations

Some *ab initio* calculations have already been performed for the phenyl peroxy radical.<sup>22–25</sup> Specifically to predict and support our spectroscopic observations, we also performed *ab initio* calculations on the phenyl peroxy radical using the GAUSSIAN 98 software package.<sup>26</sup> The optimized geometries of both the  $\tilde{A}$  and the  $\tilde{X}$  states have C<sub>s</sub> symmetry. We were able to predict the origin frequency of the  $\tilde{A}$ - $\tilde{X}$  electronic transition using two different methods, namely G2 and QCISD(T). Our *ab initio* results for T<sub>00</sub> are compared with previous calculations and our current experiment in Table 1. In addition, we calculated the vibrational frequencies for the ground and first excited electronic states, using both UHF/6-31+g(d) and B3LYP/6-31+g(d) to predict geometries and frequencies (Table 2). Qualitative descriptions of the type of motion in each vibration are also listed in Table 2. These were determined from viewing the motion of the atoms for each vibrational mode with gOpenMol software.<sup>27</sup>

## 3.2 Spectroscopic Observations

Encouraged by the relatively reproducible results of various calculations of  $T_{00}$  for the  $\tilde{A}-\tilde{X}$  transition using different computational methods, we scanned the region around  $7400\text{cm}^{-1}$  using both precursors (i.e. acetophenone and bromobenzene).

The observed spectrum is shown in Figure 1. We assigned the band at  $7497\text{cm}^{-1}$  to the electronic origin transition,  $0_0^0$ , of phenyl peroxy. This experimental value is in good agreement with our *ab initio* results given in Table 1. This spectral feature was observable using the appropriate timing (strongest for  $90\mu\text{s}$ ) between the photolysis and probe lasers, and in the presence of  $\text{O}_2$ . In addition we observed the band origin for methyl peroxy ( $\text{CH}_3\text{O}_2$ ) at  $7383\text{cm}^{-1}$ , which also results from the photodissociation of acetophenone. Comparing the experimental trace in Figure 1 with the previously reported trace for methyl peroxy<sup>13</sup> allows for easy identification of the methyl peroxy signal, and therefore assignment of the other bands in our spectrum to the phenyl peroxy signal radical.

In the spectrally congested region shown in Figure 1, we have assigned the origin and a series of sequence band in  $\nu_{33}$ . This sequence structure is expected due to the fact that the fundamental frequency of  $\nu_{33}$  is calculated to be only approximately  $85\text{cm}^{-1}$  in the  $\tilde{X}$  state, and therefore several vibrational levels should be significantly populated at room temperature. While these features are predicted to be spaced equally by about  $30\text{cm}^{-1}$ , there is an obvious anharmonicity that decreases the spacing throughout the sequence. Given that the *ab initio* calculations indicate that this sequence should be red shifted from the  $0_0^0$ , we assigned the blue-most peak to the origin.

In addition to the feature that contains the origin band in Figure 1, we have also observed a small peak with relatively sharp structure similar to the origin approximately  $230\text{cm}^{-1}$  to the blue ( $7728\text{cm}^{-1}$ ). We have assigned this to a transition from the vibrationless level of the ground state to  $\nu_{23}$  in the excited state ( $23_0^1$ ), as  $\nu_{23}$  is one of only two totally symmetric modes calculated to have fundamentals below  $1000\text{cm}^{-1}$ . Moreover unlike the other,  $\nu_{22}$  the ring C-C stretch,  $\nu_{23}$  being the Ph-O-O bend, is likely to have reasonable non-diagonal Franck-Condon activity.

The remaining feature clearly evident in Figure 1 is a broad band that appears about  $50\text{cm}^{-1}$  to the blue of the origin region. The assignment of this band is not obvious. As mentioned earlier, phenyl peroxy is expected to have only one conformer and reference to Table 2 indicate no reasonable candidate for a blue shifted vibrational band at  $\approx 50\text{cm}^{-1}$ . However also from Table 2, it is clear that this band is very near to what is expected for a transition to the  $\nu_{33}=1$  level in the  $\tilde{A}$  state. However,  $\nu_{33}$  is  $a''$  symmetry and a transition to it is not electronically allowed. Nonetheless, such a transition is vibronically allowed by first-order Herzberg-Teller coupling.<sup>28</sup> Such a Herzberg-Teller-allowed transition has not been previously

reported for any of the alkyl peroxy radicals. However, the  $\nu_{33}$  excitation could steal intensity from the  $\tilde{B}-\tilde{X}$  transition which is known to be much stronger than the  $\tilde{A}-\tilde{X}$  transition. In addition, the coupling of the  $\tilde{A}^2A'$  to the  $\tilde{B}$  (or  $\tilde{C}$ ) $^2A''$  state(s) would be expected to be much stronger in phenyl peroxy since in the alkyl peroxy radicals the  $\tilde{B}$  state is a repulsive and more than 5eV above the  $\tilde{A}$  state, while in phenyl peroxy the  $\tilde{B}$  and  $\tilde{C}$   $^2A''$  states are calculated<sup>25</sup> to be bound states in the 2.0 to 2.5eV range with one experimentally identified therein. This combination of factors should give the normally forbidden transition significant intensity. Moreover, its transition moment will be in-plane, in contrast to the allowed out-of-plane  $\tilde{A}-\tilde{X}$  transition, which could account for the very different structure of this band (compared to the origin and other allowed transitions) as one would expect a very different rotational contour for an  $a''$  vibrational band.

We also recorded the O-O stretch region, which is located approximately  $900\text{cm}^{-1}$  to the blue of the origin band, and is shown in Figure 2. There are two modes (labelled in Table 2 as  $\nu_{14}$  and  $\nu_{12}$ ) in phenyl peroxy that have O-O stretch character. Based upon our *ab initio* calculations, we have assigned the structure in the region of  $\sim 8400\text{cm}^{-1}$  to  $14_0^1$  and at  $\sim 8440\text{cm}^{-1}$  to  $12_0^1$ . Similar to the structure of the origin region, there is a  $\nu_{33}$  sequence of two or three peaks to the red of the origin of each of these O-O stretch vibrations. Additionally, we observe the broad feature about  $50\text{cm}^{-1}$  to the blue of the O-O stretch region that we assign to the Herzberg-Teller-allowed  $12_0^133_0^1$  and  $14_0^133_0^1$  transitions. The measured value of  $T_{00}$  and the determined of the  $\tilde{X}$  and  $\tilde{A}$  state frequencies are summarized in Table 3.

## 4 Conclusion

We have observed the NIR CRDS spectrum of the  $\tilde{A}^2A' - \tilde{X}^2A''$  electronic transition of the phenyl peroxy radical. This transition shows sharp vibrational structure. The spectral analysis yields  $T_{00}$  as well as determining several  $\tilde{A}$  state vibrational frequencies.

## 5 Acknowledgement

We wish to acknowledge the financial support of this work by the Chemical Sciences, Geosciences and Biosciences Division, Office of Basic Energy Sciences, Office of Science, U. S. Department of Energy, via grant DE-FG02-01ER15172.

## References

- [1] S. Wang, D. L. Miller, N. P. Cernansky, H. J. Curran, W. J. Pitz, and C. K. Westbrook, *Combust. Flame* **118**, 415 (1999).
- [2] H. J. Curran, P. Gaffuri, W. J. Pitz, and C. K. Westbrook, *Combust. Flame* **114**, 149 (1998).
- [3] C. K. Westbrook, W. J. Pitz, and W. R. Leppard, *SAE Technical Paper Series* (International Fuels and Lubricants Meeting and Exposition, Toronto, Canada, October 7-10, 1991).
- [4] P. D. Lightfoot, R. A. Cox, J. N. Crowley, M. Destriau, G. D. Hayman, M. E. Jenkins, G. K. Moortgat, and F. Zabel, *Atmos. Envir.* **26**, (1992).
- [5] T. J. Wallington, P. Dagaut, and M. J. Kurylo, *Chem. Rev.* **92**, 667 (1992).
- [6] E. P. Clifford, P. G. Wenthold, R. Gareyev, W. C. Lineberger, C. H. DePuy, V. M. Bierbaum, and G. B. Ellison, *J. Chem. Phys.* **109**, 10293 (1998).
- [7] G. J. Frost, G. B. Ellison, and V. V. and, *J. Phys. Chem. A* **103**, 10169 (1999).
- [8] B. J. Finlayson-Pitts and J. J. N. Pitts, *Science* **276**, 1045 (1997).
- [9] I. Glassman, *Combustion*, 2nd ed. (Academic Press, New York, 1986).
- [10] K. Brezinsky, *Prog. Energy Combust. Sci.* **12**, 1 (1986).
- [11] T. Yu and M. C. Lin, *J. Am. Chem. Soc.* **116**, 9571 (1994).
- [12] E. H. Fink and D. A. Ramsay, *J. Mol. Spectrosc.* **185**, 304 (1997).
- [13] M. B. Pushkarsky, S. J. Zalyubovsky, and T. A. Miller, *J. Chem. Phys.* **112**, 10695 (2000).
- [14] S. J. Zalyubovsky, D. Wang, and T. A. Miller, *Chem. Phys. Lett.* **335**, 298 (2001).
- [15] S. J. Zalyubovsky, B. G. Glover, and T. A. Miller, *J. Phys. Chem.* **107**, 7704 (2003).
- [16] S. Zalyubovsky, B. Glover, T. A. Miller, C. Hayes, J. K. Merle, and C. M. Hadad, *J. Phys. Chem.* **109**, 1308 (2005) .
- [17] L. S. Rothman, C. P. Rinsland, A. Goldman, S. T. Massie, D. P. Edwards, J. M. Flaud, A. Perrin, C. Camy-Peyret, V. Dana, J. Y. Mandin, J. Schroedera, A. McCann, R. R. Gamache, R. B. Wattson, K. Yoshino, K. V. Chance, K. W. Jucka, L. R. Brown, V. Nemtchinov, and P. Varanasi, *The HITRAN Molecular Spectroscopic Database and HAWKS (HITRAN Atmospheric Workstation)* (1996).

- [18] H.-Q. Zhao, Y.-S. Cheung, C.-L. Liao, C.-X. Liao, C. Y. Ng, and W.-K. Li, W.-K. J. Chem. Phys. **107**, 7230 (1997).
- [19] P. M. Sommeling, P. Mulder, R. Louw, D. V. Avila, J. Lusztyk, and K. U. Ingold, J. Phys. Chem. **97**, 8361 (1997).
- [20] T. Yu and M. C. Lin, J. Am. Chem. Soc. **116**, 9571 (1994).
- [21] K. Tonokura, Y. Norikane, M. Koshi, Y. Nakano, S. Nakamichi, M. Goto, S. Hashimoto, M. Kawasaki, M. P. S. Andersen, M. D. Hurley, and T. J. Wallington, J. Phys. Chem. A **106**, 5908 (2002).
- [22] M. J. Fadden, C. Barckholtz, and C. M. Hadad, J. Phys. Chem. A **104**, 3004 (2000).
- [23] A. M. Mebel and M. C. Lin, J. Am. Chem. Soc. **116**, 9977 (1994).
- [24] M. Krauss and R. Osman, J. Phys. Chem. **99**, 11387 (1995).
- [25] J. Weissman and M. Head-Gordon, J. Am. Chem. Soc. **123**, 11686 (2001).
- [26] M. J. Frisch, G. W. Trucks, H. B. Schlegel, G. E. Scuseria, M. A. Robb, J. R. Cheeseman, V. G. Zakrzewski, J. A. Montgomery, R. E. Stratmann, J. C. Burant, S. Dapprich, J. M. Millam, A. D. Daniels, K. N. Kudin, M. C. Strain, O. Farkas, J. Tomasi, V. Barone, M. Cossi, R. Cammi, B. Mennucci, C. Pomelli, C. Adamo, S. Clifford, J. Ochterski, G. A. Petersson, P. Y. Ayala, Q. Cui, K. Morokuma, D. K. Malick, A. D. Rabuck, K. Raghavachari, J. B. Foresman, J. Cioslowski, J. V. Ortiz, A. G. Baboul, B. B. Stefanov, G. Liu, A. Liashenko, P. Piskorz, I. Komaromi, R. Gomperts, R. L. Martin, D. J. Fox, T. Keith, M. A. Al-Laham, C. Y. Peng, A. Nanayakkara, C. Gonzalez, M. Challacombe, P. M. W. Gill, B. Johnson, W. Chen, M. W. Wong, J. L. andres, C. Gonzalez, M. Head-Gordon, E. S. Replogle, and J. A. Pople, *Gaussian 98, Revision A.7* (Gaussian, Inc., Pittsburgh PA, 1998).
- [27] M. Barysz, W. Duch, N. Flocke, P. Graf, N. E. Gruener, J. Karwowski, V. Kelloe, L. Laaksonen, E. S. Schreiner, N. S. Scott, M. Urban, and G. H. F. Dierksen, (The OpenMol program, version 1.31) 1997, 1998.
- [28] P. R. Bunker and P. Jensen, *Molecular Symmetry and Spectroscopy, Second Edition* (NRC Research Press, Ottawa, Ontario, Canada, 1998).

## List of Tables

1. Comparison of the  $\tilde{A}-\tilde{X}$  excitation energy  $T_{00}$  (in  $\text{cm}^{-1}$ ), determined from *ab initio* calculations and our CRDS experiment.
2. Vibrational frequencies (in  $\text{cm}^{-1}$ ) for the ground and excited states of  $\text{C}_6\text{H}_5\text{O}_2$ . Our calculated vibrational frequencies scaled by a factor of 0.9613 (as taken from NIST Computational Chemistry Comparison <http://srdata.nist.gov/cccbdb/vsf.asp>). These frequencies have been calculated after geometry optimization using B3LYP/6-31+G(D) level of theory.
3. Experimentally observed vibrational bands

## List of Figures

1. The above trace illustrates the spectrum of the  $\tilde{A} - \tilde{X}$  electronic transition of phenyl peroxy radical, produced using acetophenone as the precursor. The boxed region labelled  $\text{CH}_3\text{O}_2$  matches the previously reported experimental spectrum<sup>13</sup> of the  $\tilde{A} - \tilde{X}$  electronic transition of the methyl peroxy radical. The indicated band assignments for phenyl peroxy are discussed in the text.
2. The O-O stretch region of phenyl peroxy radical spectrum. The boxed region labelled  $\text{CH}_3\text{O}_2$  is assigned to the O-O stretch of methyl peroxy. The indicated band assignments for phenyl peroxy are discussed in the text.

Table 1: Comparison of the  $\tilde{A}-\tilde{X}$  excitation energy  $T_{00}$  (in  $\text{cm}^{-1}$ ), determined from *ab initio* calculations and our CRDS experiment.

<b>Previous and Current Work</b>	$\tilde{A} - \tilde{X}$ Transition Energy
Krauss and Osman <sup>24</sup> <i>ab initio</i> (Method: DZd-ROHF)	5501 $\text{cm}^{-1}$
Weisman and Head-Gordon <sup>25</sup> <i>ab initio</i> (Method: TDDFT)	9206 $\text{cm}^{-1}$
Present Work <i>ab initio</i> (Method: QCISD(T))	7456 $\text{cm}^{-1}$
Present <i>ab initio</i> (Method: G2)	7303 $\text{cm}^{-1}$
Present <i>ab initio</i> (Method: G2 MP2)	7324 $\text{cm}^{-1}$
Experiment	7497 $\text{cm}^{-1}$

Table 2: Vibrational frequencies (in  $\text{cm}^{-1}$ ) for the ground and excited states of  $\text{C}_6\text{H}_5\text{O}_2$ . Our calculated vibrational frequencies scaled by a factor of 0.9613 (as taken from NIST Computational Chemistry Comparison <http://srdata.nist.gov/cccbdb/vsf.asp>). These frequencies have been calculated after geometry optimization using B3LYP/6-31+G(D) level of theory.

Mode number	Vibrational Description	Symmetry	$\tilde{X}$	$\tilde{A}$
$\nu_1$	C-H Stretch	$a'$	3122	3096
$\nu_2$	C-H Stretch	$a'$	3094	3094
$\nu_3$	C-H Stretch	$a'$	3086	3086
$\nu_4$	C-H Stretch	$a'$	3075	3073
$\nu_5$	C-H Stretch	$a'$	3067	3065
$\nu_6$	C-C Stretch+C-H Wag	$a'$	1586	1583
$\nu_7$	C-C Stretch+C-H Wag	$a'$	1567	1576
$\nu_8$	C-C Stretch+C-H Wag	$a'$	1459	1466
$\nu_9$	C-C Stretch+C-H Wag	$a'$	1443	1440
$\nu_{10}$	Ring C-C Stretch	$a'$	1312	1309
$\nu_{11}$	C-H Twist	$a'$	1296	1297
$\nu_{12}$	O-O Stretch	$a'$	1161	1169
$\nu_{13}$	C-H Wag	$a'$	1144	1147
$\nu_{14}$	O-O Stretch	$a'$	1133	1141
$\nu_{15}$	C-O Stretch+C-C-H Bend	$a'$	1088	1062
$\nu_{16}$	C-C-H Bend	$a'$	1059	1008
$\nu_{17}$	C-C-H Bend	$a'$	1003	979
$\nu_{18}$	Ring Stretch	$a'$	975	966
$\nu_{19}$	C-O Stretch	$a'$	776	761
$\nu_{20}$	Ring Breathing	$a'$	600	602
$\nu_{21}$	Ring Breathing	$a'$	594	538
$\nu_{22}$	Ring C-C Stretch	$a'$	428	421
$\nu_{23}$	Ph O-O Bend	$a'$	252	213
$\nu_{24}$	C-H Wag	$a''$	962	952
$\nu_{25}$	C-C Bend	$a''$	944	928
$\nu_{26}$	Ph Wag	$a''$	890	856
$\nu_{27}$	Ph Wag	$a''$	810	793
$\nu_{28}$	C-H Bend	$a''$	736	724
$\nu_{29}$	C-C-C Bend	$a''$	659	660
$\nu_{30}$	Ph Torsion	$a''$	476	485
$\nu_{31}$	Ph Torsion	$a''$	402	399
$\nu_{32}$	Ph-C-O Wag	$a''$	225	215
$\nu_{33}$	C-C-O Wag	$a''$	85	54

Table 3: Experimentally observed vibrational bands

Observed Bands	Experimental Frequencies (in $\text{cm}^{-1}$ )	Frequencies relative to $0_0^0$
$0_0^0$	7497	0
$33_1^1$	7489	-8
$33_2^2$	7484	-13
$33_3^3$	7481	-16
$33_0^1$	7350	53
$23_0^1$	7728	213
$12_0^1$	8397	900
$14_0^1$	8441	944

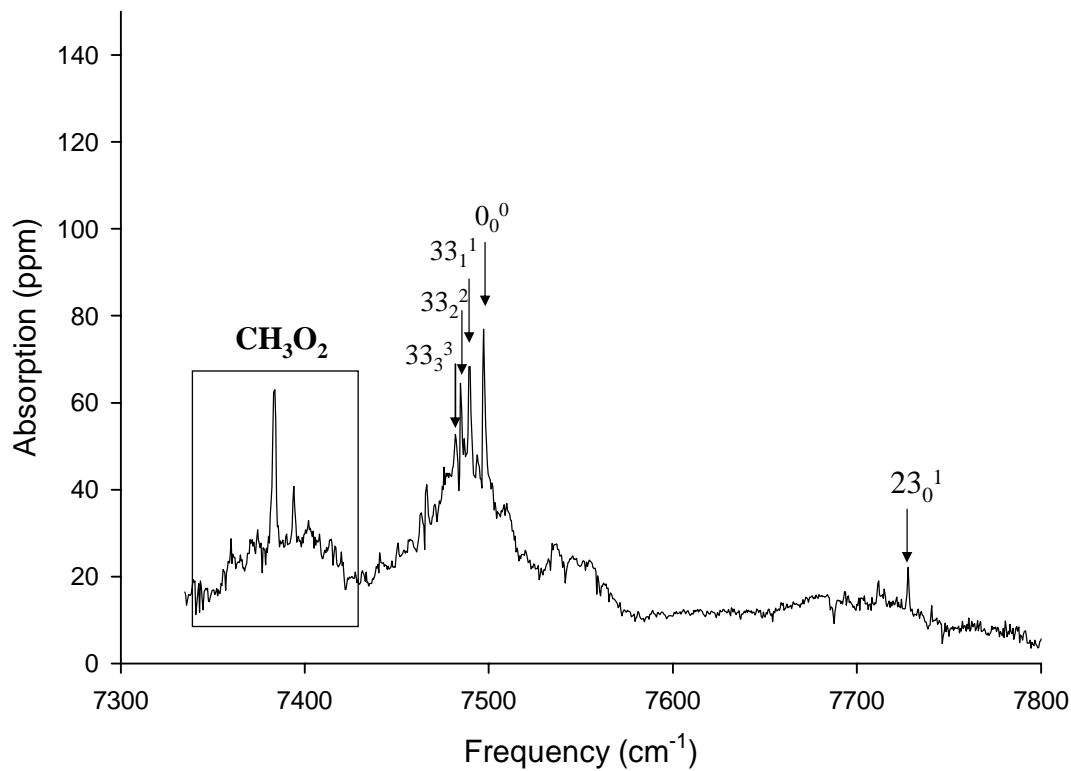


Figure 1: The above trace illustrates the spectrum of the  $\tilde{A} - \tilde{X}$  electronic transition of phenyl peroxy radical, produced using acetophenone as the precursor. The boxed region labelled  $\text{CH}_3\text{O}_2$  matches the previously reported experimental spectrum<sup>13</sup> of the  $\tilde{A} - \tilde{X}$  electronic transition of the methyl peroxy radical. The indicated band assignments for phenyl peroxy are discussed in the text.

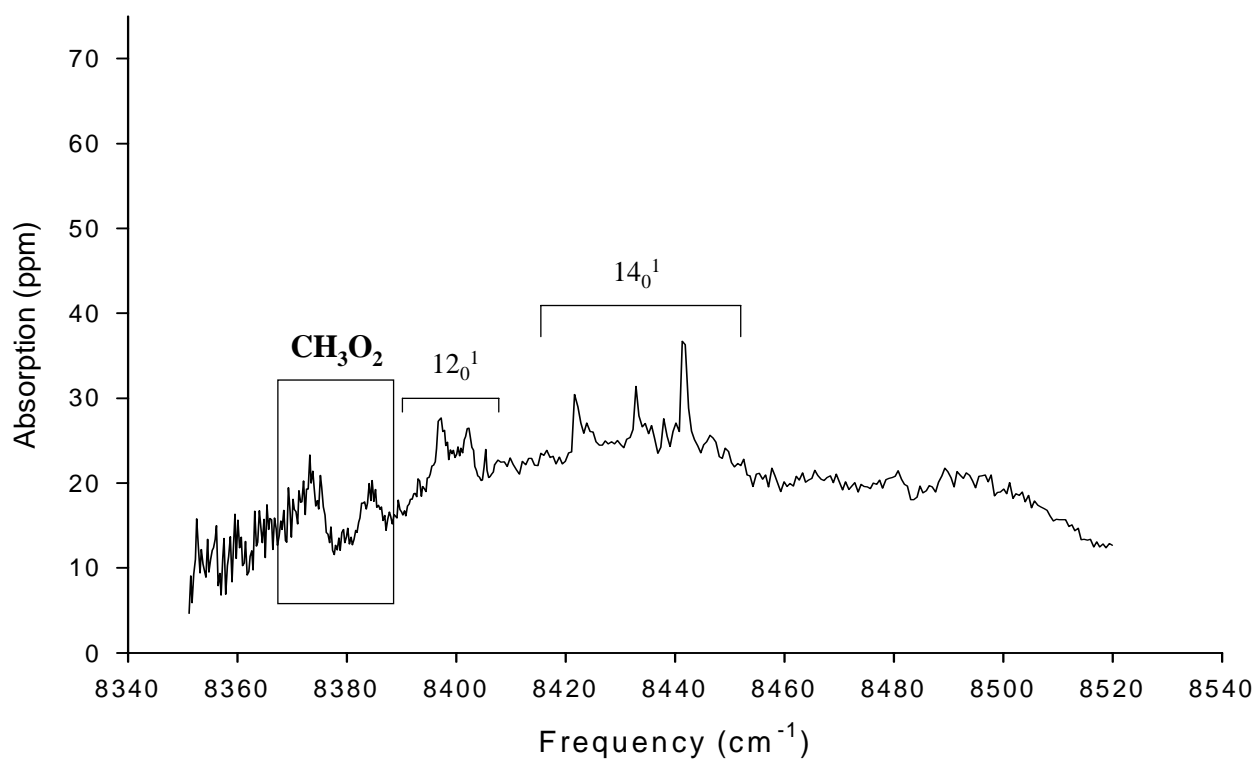


Figure 2: The O-O stretch region of phenyl peroxy radical spectrum. The boxed region labelled  $\text{CH}_3\text{O}_2$  is assigned to the O-O stretch of methyl peroxy. The indicated band assignments for phenyl peroxy are discussed in the text.